

# Active vibration isolation using a Suspension Point Interferometer

Y. Aso, M. Ando, S. Otsuka and K. Tsubono

Department of Physics, University of Tokyo, 7-3-1 Hongo Bunkyo-ku Tokyo Japan,

E-mail: aso@granite.phys.s.u-tokyo.ac.jp

**Abstract.** A suspension point interferometer (SPI) is a high-performance active vibration-isolation scheme for laser interferometric gravitational wave detectors. By making use of auxiliary interferometers installed at the suspension points of the interferometer's mirrors, this technique helps to reduce the seismic noise and to improve the stability of the interferometer. We are now constructing a Fabry-Perot interferometer equipped with an SPI to test the effectiveness of the SPI. We report on the current status of the experiment and preliminary results that demonstrate about 20 dB of vibration attenuation by the SPI below 2 Hz.

## 1. Introduction

Seismic vibration has always been a big obstacle to the interferometric detection of gravitational waves at the low frequencies; it contaminates both the sensitivity and the stability of an interferometer. Suspension point interferometer (SPI) [1] is an active vibration-isolation method that can solve both problems at the same time.

The basic idea of the SPI is to use auxiliary interferometers to monitor the seismic vibration, which induces unwanted motion to the mirrors of an interferometer. By feedback control using information from the auxiliary interferometers, we can suppress the transmission of the seismic motion.

Figure 1 (a) shows a typical configuration of an SPI installed in a Fabry-Perot interferometer, which is one arm of a Fabry-Perot-Michelson interferometer. The mirrors of the main interferometer, which is used to detect gravitational waves, are suspended from an auxiliary interferometer, called suspension point interferometer. When the SPI is locked to the laser frequency by the Pound-Drever-Hall (PDH) method [2], the two mirrors of the SPI behave together like a virtual rigid bar (Figure 1 (b)). The virtual rigid bar resists to any differential seismic motion that tries to change the length of the interferometers. In this way, one can suppress the differential seismic vibration, which induces noise indistinguishable from a gravitational wave signal to the main interferometer.

The SPI scheme has two major advantages to conventional active vibration schemes, most of which use accelerometers as sensors, low-noise nature and DC vibration attenuation ability. The low-noise feature comes from the fact that an SPI is a laser interferometer, which can be as sensitive as the main interferometer. Vibration isolation performance down to DC is available because a laser interferometer is a displacement sensor, which has the same AC and DC sensitivities, whereas the sensitivity of an accelerometer decreases as the frequency goes down.

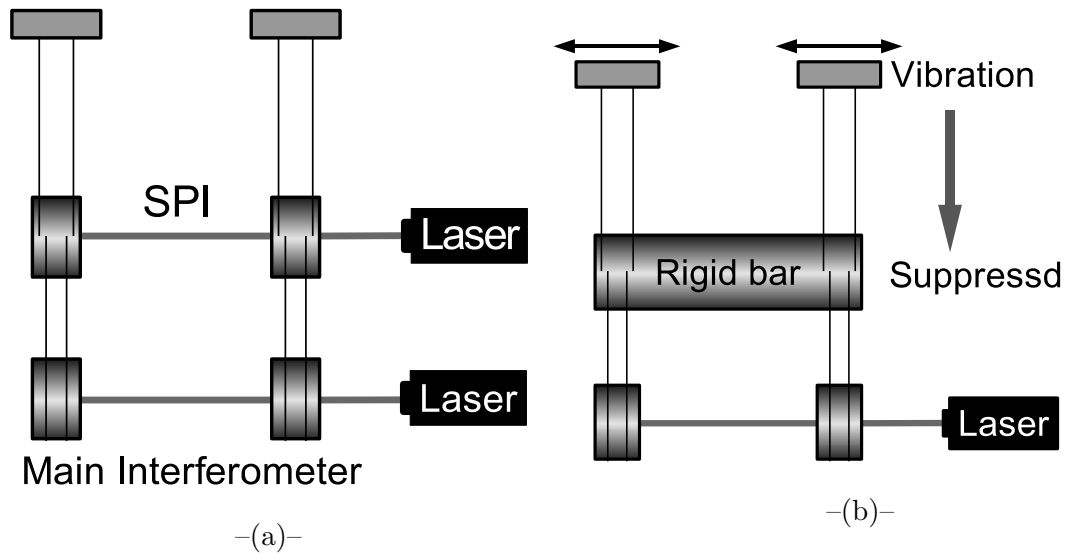


**Figure 1.** Working principle of the SPI. When the upper interferometer (SPI) is locked, that stage can be regarded as being a rigid bar. This rigid bar resists differential external disturbances.

The good DC performance enables us to reduce the residual motion of the mirrors of the main interferometer. Consequently, we can improve the stability of the interferometer. Reducing the residual motion is also expected to be helpful regarding the lock acquisition of interferometers with high-finesse arm cavities, such as resonant sideband extraction (RSE) [3] interferometers.

For Japanese next-generation interferometer LCGT (Large-scale Cryogenic Gravitational-wave Telescope) [4], SPI is not just an additional seismic attenuation layer, but a more essential component to realize a cryogenic interferometer. To cool down the mirrors of an interferometer, we have to attach heat link wires to somewhere near the main mirrors in the suspension systems<sup>1</sup>. However, these heat links introduce extra vibration to the suspension system. The SPI is used to actively suppress this extra vibration at the stage where the heat links are connected. The low-noise nature of the SPI is essential in this application, because it is placed only a few stages above the main interferometer and the vibration isolation between them is not very good; whatever noise generated in the SPI is transmitted to the main interferometer only with the poor vibration attenuation provided by the intermediate suspension stages. Therefore, we cannot use noisy sensors for this purpose.

Although an SPI can suppress differential seismic vibration, it is incapable of suppressing the common motion of its mirrors because the SPI is insusceptible to such motion. In principle, this is not a problem because the main interferometer is also insensitive to the common motion. However, in reality, some portion of the common motion at the SPI is converted to differential motion in the main interferometer due to a small asymmetry in the suspension system. This asymmetry sets a limit to the noise-reduction performance of an SPI. Various couplings from other degrees of freedom also contaminate the performance of an SPI. Therefore, an experimental test of the practical performance of the SPI is needed.

In previous work [5], we demonstrated the vibration attenuation of a Fabry-Perot interferometer by an SPI using a small (15 cm long) prototype interferometer. In this experiment, the performance of the SPI was limited by coupling from vertical vibration. We are now constructing a larger (1.5 m long) Fabry-Perot interferometer with better passive vertical

<sup>1</sup> In LCGT, we plan to attach heat links to the suspension stage directly above the main mirrors

vibration isolation mechanisms to further explore the potential of an SPI. In this paper, we report on the current status of the development of the new interferometer and preliminary results.

## 2. Experiment

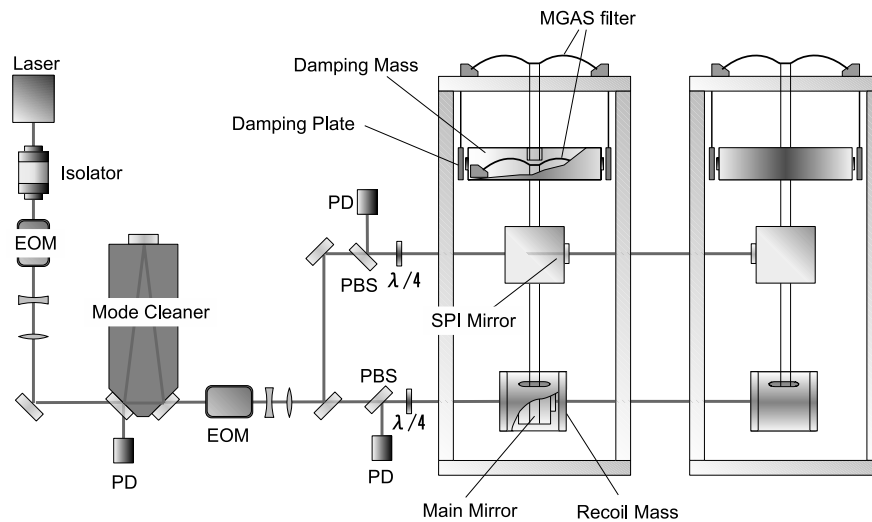


**Figure 2.** Setup of the experiment. EOM, Electro-Opto Modulator; PD, Photo Detector; PBS, Polarized Beam Splitter;  $\lambda/4$ , Quarter Wave Plate.

Our experimental setup is described schematically in figure 2. Laser light emitted from a 200 mW Nd:YAG laser is phase modulated at 40 MHz by an electro-opto modulator after passing through an optical isolator. The light is then injected to a 20 cm long triangular cavity for mode cleaning and frequency stabilization. The spacer of the triangular cavity is made of Super Invar, a very low thermal-expansion material. The finesse of the mode cleaner is about 5000. The laser frequency is locked to the cavity using the PDH method with 40 MHz phase modulation. After the mode-cleaner cavity, the laser light is phase modulated again, at 15 MHz this time. The light is then divided into two beams by a beam splitter, and each beam is led to the SPI and the main interferometer. The reflected light beams from the cavities are picked up by optical circulators formed by polarized beam splitters and quarter-wave plates, and received by photo diodes for the PDH signal acquisition.

The suspension system is basically a triple pendulum with two stages of low-frequency vertical springs, called Monolithic Geometric Anti-Spring (MGAS) filter [6]. Both MGAS filters are tuned to have a resonant frequency of 0.3 Hz.

The first stage of the suspension is called the damping mass. Strong eddy-current damping [7] is applied to this stage using attached neodymium magnets and a copper plate (damping plate) surrounding the stage for eddy-current consumption. The second stage forms the suspension point interferometer, and the final stage forms the main interferometer. Each main mirror is surrounded by a recoil mass, which is suspended from the same stage as the main mirror.

Coil-Magnet actuators are used to control the position and orientation of the suspension stages. Each stage has an actuator for horizontal position control. The damping stages and the SPI mirrors are also equipped with vertical actuators. Those vertical actuators are used to

compensate the large vertical position change caused by temperature variation, which induces the change of the equilibrium points of the MGAS filters. Horizontal actuators on the SPI and the main mirrors are used to lock the lengths of the interferometers to the laser frequency by feeding back the PDH signals. By differentially exciting the coils of an actuator, one can also control the orientation of each suspension stage.

### 3. Results and prospects

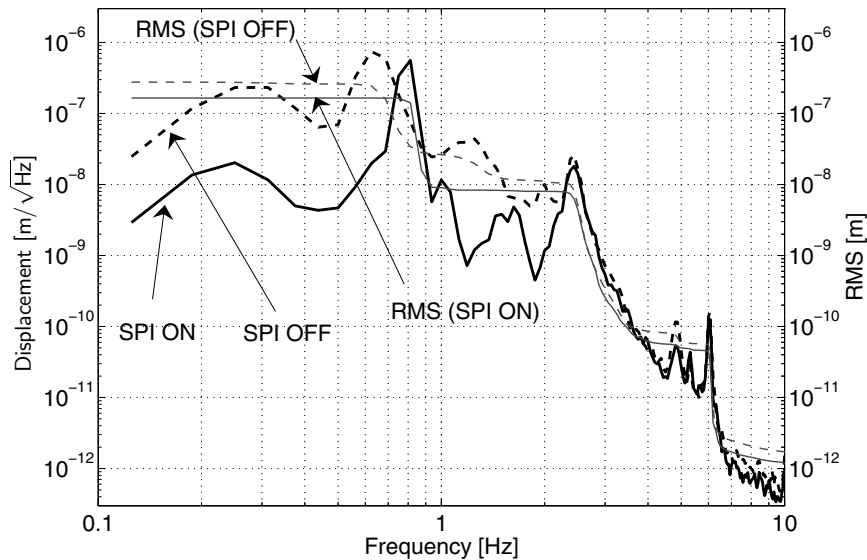


**Figure 3.** Displacement equivalent noise of the main interferometer. The thick curves are spectra of the noise. The dashed one was measured when the SPI was off and the solid one was measured when the SPI was on. The thin curves show the cumulative RMSs of the spectra.

Here, we present preliminary results from the experiment. The thick curves in figure 3 show the displacement noise spectra of the main interferometer measured with and without control of the SPI. These spectra are calibrated ones; that is, the curves do not represent the real displacement, but the calculated displacement, which is expected to occur if the PDH control is off.

Below 2 Hz, about 20 dB of noise suppression by the SPI is observed. A large peak at 0.8 Hz in the solid curve is the pendulum resonance of the main mirror, which behaves like a single pendulum suspended from a virtual rigid bar formed by the SPI. Since the virtual rigid bar isolates the main mirrors from the damping stage, this resonance has a large quality factor. However, we can easily suppress this peak, because the high quality factor resonance also provides the servo system with a high actuation efficiency at exactly the same frequency. Therefore, this peak does not harm the stability of the main interferometer. Above 2 Hz, the two curves are almost identical; no noise suppression by the SPI can be observed. We think that this is mainly because of the couplings from other degrees of freedom, such as pitch motion. Especially, a peak at 2.5 Hz was identified to be the pitch resonance of the main mirrors. A sharp peak at 6 Hz is the pitch resonance of the SPI mirrors.

The thin curves in figure 3 show the cumulative root-mean-squares (RMSs) of the interferometer's noise, which are calculated by integrating the spectra over the shown frequency

range (0.1 - 10 Hz). The overall RMS without the SPI is  $2.8 \times 10^{-7}$  m, whereas the one with the SPI is  $1.6 \times 10^{-7}$  m; the RMS was nearly reduced by half. As seen in the figure, the RMS with the SPI is dominated by the peak at 0.8 Hz, which, however, does not really make the interferometer unstable as explained above.

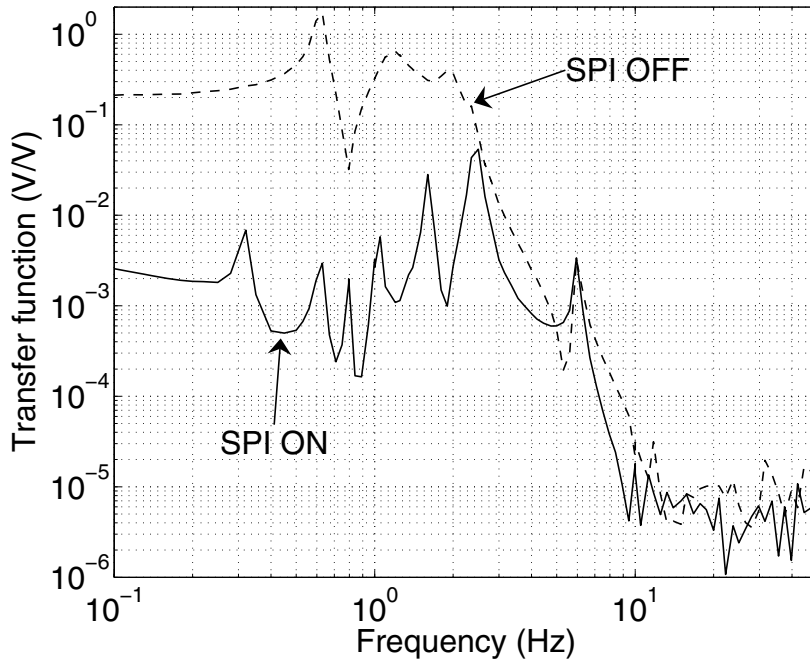


**Figure 4.** Transfer functions from a damping mass to the main interferometer. The dashed curve was measured when the SPI was off. The solid curve was measured when the SPI was on

Figure 4 shows the transfer functions from the excitation voltage applied to the horizontal actuator of a damping stage to the feedback signal of the main interferometer. The two curves represent measurements with and without control of the SPI. Over 40 dB suppression of vibration transfer has been observed below 2 Hz. Around 10 Hz, we still have about 20 dB of suppression by the SPI. Above 10 Hz, because the passive vibration isolation was very good, we could not sufficiently excite the damping stage to measure the transfer function. Like the noise-spectrum measurements, the pitch resonance of the SPI mirrors at 6 Hz contaminates this measurement.

The pitch resonances of the SPI and main mirrors are the main obstacles that limit the performance of the SPI so far. Therefore, we are now making modifications to the suspension systems to lower the pitch resonant frequencies. The modifications include narrowing the distances between the wire clamp points on the SPI mirrors in the direction of their thickness and adding extra masses to the main mirrors to increase their moment of inertia. After those modifications, we expect that the noise suppression by the SPI in spectrum will be observed over a wider frequency range. We also expect that a removal of the 6 Hz peak in the transfer functions will provide a clearer demonstration of transfer function improvement by the SPI.

#### Acknowledgments

The authors are grateful to Riccardo DeSalvo for helping us to design and manufacture the MGAS filters.

A part of this research is supported by a Grant-in-Aid for JSPS Fellows and a Grant-in-Aid for Scientific Research on Priority Areas (415) of the Ministry of Education, Culture, Sports, Science and Technology.

## References

- [1] R.W.P. Drever, Outline of a proposed design for a first receiver for installation in the long-baseline facilities of Fabry-Perot type, *LIGO Document T870001-00-R*, 1987.
- [2] R.W.P. Drever, J.L. Hall, F.V. Kowalski, J. Hough, G.M. Ford, A.J. Munley, H. Ward, *Appl. Phys. B* **31** (1983) 97.
- [3] J. Mizuno, K.A. Strain, P.G. Nelson, J.M. Chen, R. Schilling, A. Rüdiger, W. Winkler, K. Danzmann, *Phys. Lett. A* **175** (1993) 273.
- [4] K. Kuroda, *et. al.*, *Classical Quant. Grav.* **20** (2003) 871.
- [5] Y. Aso, M. Ando, K. Kawabe, S. Otsuka, K. Tsubono, *Phys. Lett. A* **327** (2004) 1.
- [6] G. Cella, R. DeSalvo, V. Sannibale, H. Tariq, N. Viboud, A. Takamori, *Nucl. Instrum. Meth. A* **487** (2002) 652.
- [7] K. Tsubono, A. Araya, K. Kawabe, S. Moriwaki, N. Mio, *Rev. Sci. Instrum.* **64** (1993) 2237.